Observation of the Decay $D^0 \to K^-\pi^+e^+e^-$

J. P. Lees,[1] V. Poireau,[1] V. Tisserand,[1] E. Grauges,[2] A. Palano,[3] G. Eigen,[4] D. N. Brown,[5] Yu. G. Kolomensky,[5] M. Fritsch,[6] H. Koch,[6] T. Schroeder,[6] C. Hearty,[7a,7b] T. S. Mattison,[7b] J. A. McKenna,[7b] R. Y. So,[7b] V. E. Blinov,[8a,8b,8c] A. R. Buzykaev,[8a] V. P. Druzhinin,[8a,8b] V. B. Golubev,[8a,8b] E. A. Kozyrev,[8a,8b] E. A. Kravchenko,[8a,8b] A. P. Onuchin,[8a,8b,8c] S. I. Serednyakov,[8a,8b] Yu. I. Skovpen,[8a,8b] E. P. Solodov,[8a,8b] K. Yu. Todyshev,[8a,8b] A. J. Lankford,[9] J. W. Gary,[10] O. Long,[10] A. M. Eisner,[11] W. S. Lockman,[11] W. Panduro Vazquez,[11] D. S. Chao,[12] C. H. Cheng,[12] B. Echenard,[12] K. T. Flood,[12] D. G. Hitlin,[12] J. Kim,[12] Y. Li,[12] T. S. Miyashita,[12] P. Ongmongkolkul,[12] F. C. Porter,[12] M. Röhrken,[12] Z. Huard,[13] B. T. Meadows,[13] B. G. Pushpawela,[13] M. D. Sokoloff,[13] L. Sun,[13,†] J. G. Smith,[14] S. R. Wagner,[14] D. Bernard,[15] M. Verderi,[15] D. Bettoni,[16a] C. Bozzi,[16a] R. Calabrese,[16a,16b] G. Cibinetto,[16a,16b] E. Fioravanti,[16a,16b] I. Garzia,[16a,16b] E. Luppi,[16a,16b] V. Santoro,[16a] A. Calcaterra,[17] R. de Sangro,[17] G. Finocchiaro,[17] S. Martellotti,[17] P. Patteri,[17] I. M. Peruzzi,[17] M. Piccolo,[17] M. Rotondo,[17] A. Zallo,[17] S. Passaggio,[18] C. Patrignani,[18,‡] H. M. Lacker,[19] B. Bhuyan,[20] U. Mallik,[21] C. Chen,[22] J. Cochran,[22] S. Prell,[22] A. V. Gritsan,[23] N. Arnaud,[24] M. Davier,[24] F. Le Diberder,[24] A. M. Lutz,[24] G. Wormser,[24] D. J. Lange,[25] D. M. Wright,[25] J. P. Coleman,[26] E. Gabathuler,[26,*] D. E. Hutchcroft,[26] D. J. Payne,[26] C. Touramanis,[26] A. J. Bevan,[27] F. Di Lodovico,[27] R. Sacco,[27] G. Cowan,[28] Sw. Banerjee,[29] D. N. Brown,[29] C. L. Davis,[29] A. G. Denig,[30] W. Gradl,[30] K. Griessinger,[30] A. Hafner,[30] K. R. Schubert,[30] R. J. Barlow,[31,§] G. D. Lafferty,[31] R. Cenci,[32] A. Jawahery,[32] D. A. Roberts,[32] R. Cowan,[33] S. H. Robertson,[34a,34b] R. M. Seddon,[34b] B. Dey,[35a] N. Neri,[35a] F. Palombo,[35a,35b] R. Cheaib,[36] L. Cremaldi,[36] R. Godang,[36,¶] D. J. Summers,[36] P. Taras,[37] G. De Nardo,[38] C. Sciacca,[38] G. Raven,[39] C. P. Jessop,[40] J. M. LoSecco,[40] K. Honscheid,[41] R. Kass,[41] A. Gaz,[42a] M. Margoni,[42a,42b] M. Posocco,[42a] G. Simi,[42a,42b] F. Simonetto,[42a,42b] R. Stroili,[42a,42b] S. Akar,[43] E. Ben-Haim,[43] M. Bomben,[43] G. R. Bonneaud,[43] G. Calderini,[43] J. Chauveau,[43] G. Marchiori,[43] J. Ocariz,[43] M. Biasini,[44a,44b] E. Manoni,[44a] A. Rossi,[44a] G. Batignani,[45a,45b] S. Bettarini,[45a,45b] M. Carpinelli,[45a,45b,**] G. Casarosa,[45a,45b] M. Chrzaszcz,[45a] F. Forti,[45a,45b] M. A. Giorgi,[45a,45b] A. Lusiani,[45a,45c] B. Oberhof,[45a,45b] E. Paoloni,[45a,45b] M. Rama,[45a] G. Rizzo,[45a,45b] J. J. Walsh,[45a] L. Zani,[45a,45b] A. J. S. Smith,[46] F. Anulli,[47a] R. Faccini,[47a,47b] F. Ferrarotto,[47a] F. Ferroni,[47a,47b] A. Pilloni,[47a,47b] G. Piredda,[47a,*] C. Bünger,[48] S. Dittrich,[48] O. Grünberg,[48] M. Heß,[48] T. Leddig,[48] C. Voß,[48] R. Waldi,[48] T. Adye,[49] F. F. Wilson,[49] S. Emery,[50] G. Vasseur,[50] D. Aston,[51] C. Cartaro,[51] M. R. Convery,[51] J. Dorfan,[51] W. Dunwoodie,[51] M. Ebert,[51] R. C. Field,[51] B. G. Fulsom,[51] M. T. Graham,[51] C. Hast,[51] W. R. Innes,[51,*] P. Kim,[51] D. W. G. S. Leith,[51] S. Luitz,[51] D. B. MacFarlane,[51] D. R. Muller,[51] H. Neal,[51] B. N. Ratcliff,[51] A. Roodman,[51] M. K. Sullivan,[51] J. Va'vra,[51] W. J. Wisniewski,[51] M. V. Purohit,[52] J. R. Wilson,[52] A. Randle-Conde,[53] S. J. Sekula,[53] H. Ahmed,[54] M. Bellis,[55] P. R. Burchat,[55] E. M. T. Puccio,[55] M. S. Alam,[56] J. A. Ernst,[56] R. Gorodeisky,[57] N. Guttman,[57] D. R. Peimer,[57] A. Soffer,[57] S. M. Spanier,[58] J. L. Ritchie,[59] R. F. Schwitters,[59] J. M. Izen,[60] X. C. Lou,[60] F. Bianchi,[61a,61b] F. De Mori,[61a,61b] A. Filippi,[61a] D. Gamba,[61a,61b] L. Lanceri,[62] L. Vitale,[62] F. Martinez-Vidal,[63] A. Oyanguren,[63] J. Albert,[64b] A. Beaulieu,[64b] F. U. Bernlochner,[64b] G. J. King,[64b] R. Kowalewski,[64b] T. Lueck,[64b] I. M. Nugent,[64b] J. M. Roney,[64b] R. J. Sobie,[64a,64b] N. Tasneem,[64b] T. J. Gershon,[65] P. F. Harrison,[65] T. E. Latham,[65] R. Prepost,[66] and S. L. Wu[66]

(*BABAR* Collaboration)

[1]*Laboratoire d'Annecy-le-Vieux de Physique des Particules (LAPP), Université de Savoie, CNRS/IN2P3, F-74941 Annecy-Le-Vieux, France*
[2]*Universitat de Barcelona, Facultat de Fisica, Departament ECM, E-08028 Barcelona, Spain*
[3]*INFN Sezione di Bari and Dipartimento di Fisica, Università di Bari, I-70126 Bari, Italy*
[4]*University of Bergen, Institute of Physics, N-5007 Bergen, Norway*
[5]*Lawrence Berkeley National Laboratory and University of California, Berkeley, California 94720, USA*
[6]*Ruhr Universität Bochum, Institut für Experimentalphysik 1, D-44780 Bochum, Germany*
[7a]*Institute of Particle Physics, Vancouver, British Columbia, Canada V6T 1Z1*
[7b]*University of British Columbia, Vancouver, British Columbia, Canada V6T 1Z1*
[8a]*Budker Institute of Nuclear Physics SB RAS, Novosibirsk 630090, Russia*
[8b]*Novosibirsk State University, Novosibirsk 630090, Russia*
[8c]*Novosibirsk State Technical University, Novosibirsk 630092, Russia*
[9]*University of California at Irvine, Irvine, California 92697, USA*
[10]*University of California at Riverside, Riverside, California 92521, USA*
[11]*University of California at Santa Cruz, Institute for Particle Physics, Santa Cruz, California 95064, USA*
[12]*California Institute of Technology, Pasadena, California 91125, USA*

[13]University of Cincinnati, Cincinnati, Ohio 45221, USA
[14]University of Colorado, Boulder, Colorado 80309, USA
[15]Laboratoire Leprince-Ringuet, Ecole Polytechnique, CNRS/IN2P3, F-91128 Palaiseau, France
[16a]INFN Sezione di Ferrara, I-44122 Ferrara, Italy
[16b]Dipartimento di Fisica e Scienze della Terra, Università di Ferrara, I-44122 Ferrara, Italy
[17]INFN Laboratori Nazionali di Frascati, I-00044 Frascati, Italy
[18]INFN Sezione di Genova, I-16146 Genova, Italy
[19]Humboldt-Universität zu Berlin, Institut für Physik, D-12489 Berlin, Germany
[20]Indian Institute of Technology Guwahati, Guwahati, Assam, 781 039, India
[21]University of Iowa, Iowa City, Iowa 52242, USA
[22]Iowa State University, Ames, Iowa 50011, USA
[23]Johns Hopkins University, Baltimore, Maryland 21218, USA
[24]Laboratoire de l'Accélérateur Linéaire, IN2P3/CNRS et Université Paris-Sud 11, Centre Scientifique d'Orsay, F-91898 Orsay Cedex, France
[25]Lawrence Livermore National Laboratory, Livermore, California 94550, USA
[26]University of Liverpool, Liverpool L69 7ZE, United Kingdom
[27]Queen Mary, University of London, London, E1 4NS, United Kingdom
[28]University of London, Royal Holloway and Bedford New College, Egham, Surrey TW20 0EX, United Kingdom
[29]University of Louisville, Louisville, Kentucky 40292, USA
[30]Johannes Gutenberg-Universität Mainz, Institut für Kernphysik, D-55099 Mainz, Germany
[31]University of Manchester, Manchester M13 9PL, United Kingdom
[32]University of Maryland, College Park, Maryland 20742, USA
[33]Massachusetts Institute of Technology, Laboratory for Nuclear Science, Cambridge, Massachusetts 02139, USA
[34a]Institute of Particle Physics, Montréal, Québec, Canada H3A 2T8
[34b]McGill University, Montréal, Québec, Canada H3A 2T8
[35a]INFN Sezione di Milano, I-20133 Milano, Italy
[35b]Dipartimento di Fisica, Università di Milano, I-20133 Milano, Italy
[36]University of Mississippi, University, Mississippi 38677, USA
[37]Université de Montréal, Physique des Particules, Montréal, Québec, Canada H3C 3J7
[38]INFN Sezione di Napoli and Dipartimento di Scienze Fisiche, Università di Napoli Federico II, I-80126 Napoli, Italy
[39]NIKHEF, National Institute for Nuclear Physics and High Energy Physics, NL-1009 DB Amsterdam, The Netherlands
[40]University of Notre Dame, Notre Dame, Indiana 46556, USA
[41]Ohio State University, Columbus, Ohio 43210, USA
[42a]INFN Sezione di Padova, I-35131 Padova, Italy
[42b]Dipartimento di Fisica, Università di Padova, I-35131 Padova, Italy
[43]Laboratoire de Physique Nucléaire et de Hautes Energies, IN2P3/CNRS, Université Pierre et Marie Curie-Paris6, Université Denis Diderot-Paris7, F-75252 Paris, France
[44a]INFN Sezione di Perugia, I-06123 Perugia, Italy
[44b]Dipartimento di Fisica, Università di Perugia, I-06123 Perugia, Italy
[45a]INFN Sezione di Pisa, I-56127 Pisa, Italy
[45b]Dipartimento di Fisica, Università di Pisa, I-56127 Pisa, Italy
[45c]Scuola Normale Superiore di Pisa, I-56127 Pisa, Italy
[46]Princeton University, Princeton, New Jersey 08544, USA
[47a]INFN Sezione di Roma, I-00185 Roma, Italy
[47b]Dipartimento di Fisica, Università di Roma La Sapienza, I-00185 Roma, Italy
[48]Universität Rostock, D-18051 Rostock, Germany
[49]Rutherford Appleton Laboratory, Chilton, Didcot, Oxon, OX11 0QX, United Kingdom
[50]CEA, Irfu, SPP, Centre de Saclay, F-91191 Gif-sur-Yvette, France
[51]SLAC National Accelerator Laboratory, Stanford, California 94309 USA
[52]University of South Carolina, Columbia, South Carolina 29208, USA
[53]Southern Methodist University, Dallas, Texas 75275, USA
[54]St. Francis Xavier University, Antigonish, Nova Scotia, Canada B2G 2W5
[55]Stanford University, Stanford, California 94305, USA
[56]State University of New York, Albany, New York 12222, USA
[57]Tel Aviv University, School of Physics and Astronomy, Tel Aviv, 69978, Israel
[58]University of Tennessee, Knoxville, Tennessee 37996, USA
[59]University of Texas at Austin, Austin, Texas 78712, USA
[60]University of Texas at Dallas, Richardson, Texas 75083, USA
[61a]INFN Sezione di Torino, I-10125 Torino, Italy
[61b]Dipartimento di Fisica, Università di Torino, I-10125 Torino, Italy

[62]INFN Sezione di Trieste and Dipartimento di Fisica, Università di Trieste, I-34127 Trieste, Italy
[63]IFIC, Universitat de Valencia-CSIC, E-46071 Valencia, Spain
[64a]Institute of Particle Physics, Canada V8W 3P6
[64b]University of Victoria, Victoria, British Columbia, Canada V8W 3P6
[65]Department of Physics, University of Warwick, Coventry CV4 7AL, United Kingdom
[66]University of Wisconsin, Madison, Wisconsin 53706, USA

(Received 30 August 2018; revised manuscript received 11 December 2018; published 27 February 2019)

We report the observation of the rare charm decay $D^0 \to K^-\pi^+e^+e^-$, based on 468 fb^{-1} of e^+e^- annihilation data collected at or close to the center-of-mass energy of the $\Upsilon(4S)$ resonance with the *BABAR* detector at the SLAC National Accelerator Laboratory. We find the branching fraction in the invariant mass range $0.675 < m(e^+e^-) < 0.875$ GeV/c^2 of the electron-positron pair to be $\mathcal{B}(D^0 \to K^-\pi^+e^+e^-) = (4.0 \pm 0.5 \pm 0.2 \pm 0.1) \times 10^{-6}$, where the first uncertainty is statistical, the second systematic, and the third due to the uncertainty in the branching fraction of the decay $D^0 \to K^-\pi^+\pi^+\pi^-$ used as a normalization mode. The significance of the observation corresponds to 9.7 standard deviations including systematic uncertainties. This result is consistent with the recently reported $D^0 \to K^-\pi^+\mu^+\mu^-$ branching fraction, measured in the same invariant mass range, and with the value expected in the standard model. In a set of regions of $m(e^+e^-)$, where long-distance effects are potentially small, we determine a 90% confidence level upper limit on the branching fraction $\mathcal{B}(D^0 \to K^-\pi^+e^+e^-) < 3.1 \times 10^{-6}$.

DOI: 10.1103/PhysRevLett.122.081802

The decay $D^0 \to K^-\pi^+e^+e^-$ [1] is expected to be very rare in the standard model (SM) as it cannot occur at tree level [2]. Short-distance contributions to the $D^0 \to K^-\pi^+e^+e^-$ branching fraction proceed through loop and box diagrams [3] and are expected to be $\mathcal{O}(10^{-9})$. However, decays with long-distance contributions, such as $D^0 \to VX$, where V is a vector or pseudoscalar meson decaying to two leptons and X is an accompanying particle or particles, could contribute at the level of $\mathcal{O}(10^{-6})$ through photon pole amplitudes or vector meson dominance [3–7].

Certain physics models beyond the standard model, such as minimal supersymmetric or R-parity-violating supersymmetric theories, predict branching fractions as high as $\mathcal{O}(10^{-5})$ [3,7–10]. As virtual particles can enter in the one-loop processes, this type of decay can be used to study new physics processes at large mass scales. These processes could potentially be detected in regions where the decays of intermediate mesons do not dominate.

Over the last few years there have been a number of measurements of the decays of B mesons to final states involving one or more charged leptons. Some of these measurements suggest a possible deviation from the assumption that all leptons couple equally [11–20]. The possibility therefore exists that a deviation from lepton universality will be seen in D meson decays.

Recently, the LHCb Collaboration measured $\mathcal{B}(D^0 \to K^-\pi^+\mu^+\mu^-) = (4.17 \pm 0.12 \pm 0.40) \times 10^{-6}$ in the mass range $0.675 < m(\mu^+\mu^-) < 0.875$ GeV/c^2, where the decay is dominated by the ρ^0 and ω resonances [21]. For modes involving electrons, the CLEO Collaboration set 90% confidence level (C.L.) limits on the branching fractions $\mathcal{B}(D^0 \to X\ell^+\ell^-)$ in the range $(4.5–118) \times 10^{-5}$, where X represents a π^0, K^0_S, η, ρ^0, ω, or ϕ meson and $\ell = e$ or μ [22]. The E791 Collaboration has reported $\mathcal{B}(D^0 \to K^-\pi^+e^+e^-) < 38.5 \times 10^{-5}$ at the 90% C.L. in the full $m(K^-\pi^+)$ invariant mass range and $\mathcal{B}(D^0 \to K^-\pi^+e^+e^-) < 4.7 \times 10^{-5}$ in the $m(K^-\pi^+)$ mass range within 55 MeV/c^2 of the $\bar{K}^*(892)^0$ mass [23,24].

We report here the observation of the decay $D^0 \to K^-\pi^+e^+e^-$ [1] with data recorded with the *BABAR* detector at the PEP-II asymmetric-energy e^+e^- collider operated at the SLAC National Accelerator Laboratory. The data sample corresponds to 424 fb^{-1} of e^+e^- collisions collected at the center-of-mass energy of the $\Upsilon(4S)$ resonance (on peak) and an additional 44 fb^{-1} of data collected 40 MeV below the $\Upsilon(4S)$ resonance (off peak) [25]. The signal branching fraction $\mathcal{B}(D^0 \to K^-\pi^+e^+e^-)$ is measured relative to the normalization decay $D^0 \to K^-\pi^+\pi^+\pi^-$. The D^0 mesons are reconstructed from the decay $D^{*+} \to D^0\pi^+$ produced in $e^+e^- \to c\bar{c}$ events. The use of this decay chain increases the purity of the sample at the expense of a smaller number of reconstructed D^0 mesons.

The *BABAR* detector is described in detail in Ref. [26]. Charged particles are reconstructed as tracks with a five-layer silicon vertex detector and a 40-layer drift chamber inside a 1.5 T solenoidal magnet. An electromagnetic calorimeter comprised of 6580 CsI(Tl) crystals is used

to identify electrons and photons. A ring-imaging Cherenkov detector is used to identify charged hadrons and to provide additional lepton identification information. Muons are identified with an instrumented magnetic-flux return.

Monte Carlo (MC) simulation is used to evaluate the level of background contamination and selection efficiencies. Simulated events are also used to cross-check the selection procedure and for studies of systematic effects. The signal and normalization channels are simulated with the EvtGen package [27]. We generate the signal channel decay with a phase-space model, while the normalization mode includes two-body and three-body intermediate resonances, as well as nonresonant decays. For background studies, we generate $e^+e^- \to q\bar{q}$ ($q = u, d, s, c$), dimuon, Bhabha elastic e^+e^- scattering, $B\bar{B}$ background, and two-photon events [28,29]. The background samples are produced with an integrated luminosity approximately 6 times that of the data. Final-state radiation is provided by PHOTOS [30]. The detector response is simulated with GEANT4 [31,32]. All simulated events are reconstructed in the same manner as the data.

Events are required to contain at least five charged tracks. Candidate D^0 mesons are formed from four charged tracks reconstructed with the appropriate mass hypothesis for the $D^0 \to K^-\pi^+e^+e^-$ and $D^0 \to K^-\pi^+\pi^+\pi^-$ decays. Particle identification (PID) is applied to the charged tracks and the same criteria are applied to the signal and normalization modes [26,33]. The four tracks must form a good-quality vertex with a χ^2 probability for the vertex fit greater than 0.005. In the case of $D^0 \to K^-\pi^+e^+e^-$, a bremsstrahlung energy recovery algorithm is applied to the electrons, in which the energy of photon showers that are within a small angle (typically 35 mrad) of the initial electron direction are added to the energy of the electron candidate. The electron-positron pair must have an invariant mass $m(e^+e^-) > 0.1$ GeV/c^2. The D^0 candidate momentum in the PEP-II center-of-mass system p^* must be greater than 2.4 GeV/c. The requirement for five charged tracks strongly suppresses backgrounds from QED processes. The p^* criterion removes most sources of combinatorial background and also charm hadrons produced in B decays, which are kinematically limited to less than ~2.2 GeV/c.

The candidate D^{*+} is formed by combining the D^0 candidate with a charged pion with a momentum in the laboratory frame greater than 0.1 GeV/c. The pion is required to have a charge opposite to that of the kaon in the D^0 decay. A vertex fit is performed with the D^0 mass constrained to its known value and the requirement that the D^0 meson and the pion originate from the interaction region. The χ^2 probability of the fit is required to be greater than 0.005. The D^0 meson mass $m(D^0)$ must be in the range $1.81 < m(D^0) < 1.91$ GeV/c^2 and the mass difference, $\Delta m = m(D^{*+}) - m(D^0)$, between the reconstructed masses of the D^{*+} and D^0 candidates is required to satisfy $0.143 < \Delta m < 0.148$ GeV/c^2. The regions around the peak positions in $m(D^0)$ and Δm in data are kept hidden until the analysis steps are finalized.

To reject misreconstructed $D^0 \to K^-\pi^+e^+e^-$ candidates that originate from D^0 hadronic decays with large branching fractions where one or more charged tracks are misidentified by the PID the candidate is reconstructed assuming the kaon or pion mass hypothesis for the leptons. If the resulting candidate $m(D^0)$ is within 20 MeV/c^2 of the known D^0 mass [34] and $|\Delta m| < 2$ MeV/c^2, the event is discarded. After these criteria are applied, the background from these hadronic decays is negligible. Multiple candidates occur in less than 4% of simulated $D^0 \to K^-\pi^+\pi^+\pi^-$ decays and in less than 2% of $D^0 \to K^-\pi^+e^+e^-$ decays. If two or more candidates are found in an event, the one with the highest vertex χ^2 probability is selected.

After the application of all selection criteria and corrections for small differences between data and MC simulation in tracking and PID performance, the average reconstruction efficiency for the $D^0 \to K^-\pi^+\pi^+\pi^-$ decay is $\hat{\epsilon}_{\rm norm} = (20.1 \pm 0.2)\%$, where the uncertainty is due to the limited size of the simulation sample. For the $D^0 \to K^-\pi^+e^+e^-$ decay, the average reconstruction efficiency $\hat{\epsilon}_{\rm sig}$ varies between 5.0% and 8.9% depending on the $m(e^+e^-)$ mass range. The remaining background comes predominantly from $e^+e^- \to c\bar{c}$ events. No evidence is found in MC simulation for backgrounds that peak in the $m(D^0)$ and Δm signal region.

The $D^0 \to K^-\pi^+e^+e^-$ branching fraction is determined relative to that of the normalization decay channel $D^0 \to K^-\pi^+\pi^+\pi^-$ using

$$\frac{\mathcal{B}(D^0 \to K^-\pi^+e^+e^-)}{\mathcal{B}(D^0 \to K^-\pi^+\pi^+\pi^-)} = \frac{\hat{\epsilon}_{\rm norm}}{N_{\rm norm}} \frac{\mathcal{L}_{\rm norm}}{\mathcal{L}_{\rm sig}} \sum_i^{N_{\rm sig}} \frac{1}{\epsilon_{\rm sig}^i}, \quad (1)$$

where $\mathcal{B}(D^0 \to K^-\pi^+\pi^+\pi^-)$ is the branching fraction of the normalization mode [34], and $N_{\rm norm}$ and $\hat{\epsilon}_{\rm norm}$ are the $D^0 \to K^-\pi^+\pi^+\pi^-$ fitted yield and the reconstruction efficiency calculated from simulated $D^0 \to K^-\pi^+\pi^+\pi^-$ decays, respectively. The fitted $D^0 \to K^-\pi^+e^+e^-$ signal yield is represented by $N_{\rm sig}$, and $\epsilon_{\rm sig}^i$ is the reconstruction efficiency for each signal candidate i, calculated from MC simulated $D^0 \to K^-\pi^+e^+e^-$ decays as a function of $m(e^+e^-)$ and $m(K^-\pi^+)$. The symbols $\mathcal{L}_{\rm sig}$ and $\mathcal{L}_{\rm norm}$ represent the integrated luminosities used for the signal $D^0 \to K^-\pi^+e^+e^-$ decay (468.2 ± 2.0 fb^{-1}) and the normalization $D^0 \to K^-\pi^+\pi^+\pi^-$ decay (39.3 ± 0.2 fb^{-1}), respectively [25]. The signal mode uses both the on-peak and off-peak data samples while the normalization mode uses only a subset of the off-peak data.

The $D^0 \to K^-\pi^+e^+e^-$ and $D^0 \to K^-\pi^+\pi^+\pi^-$ yields are determined from extended unbinned maximum likelihood fits to the Δm and the four-body mass distributions. The

Δm and the four-body mass distributions are not correlated and are treated as independent observables in the fit. For the $D^0 \to K^-\pi^+e^+e^-$ signal, a Gaussian-like function with different lower and upper widths is used for both Δm and $m(K^-\pi^+e^+e^-)$. This asymmetric function is used in order to describe the imperfect bremsstrahlung energy recovery for the electrons. The background in the $D^0 \to K^-\pi^+e^+e^-$ channel is modeled with an ARGUS threshold function [35] for Δm and a first-order Chebyshev polynomial for $m(K^-\pi^+e^+e^-)$. For the $D^0 \to K^-\pi^+\pi^+\pi^-$ normalization mode, the Δm and $m(K^-\pi^+\pi^-\pi^+)$ distributions are each represented by two Cruijff functions with shared means [36]. The background is represented by an ARGUS threshold function for Δm and a second-order Chebyshev polynomial for $m(K^-\pi^+\pi^-\pi^+)$. All yields and shape parameters are allowed to vary in the fits except for the ARGUS function threshold end point, which is set to the kinematic threshold for the $D^{*+} \to D^0\pi^+$ decay.

Decays of intermediate mesons to the final state $e^+e^-\gamma$ can potentially appear in the $m(e^+e^-)$ spectrum as the photon is not reconstructed. However, the constraint $m(D^0) > 1.81\ \mathrm{GeV}/c^2$ is effective in reducing the background from these decays despite their relatively high branching fractions. We investigate the backgrounds by generating simulation samples $D^0 \to K^-\pi^+V$, with intermediate decays $\rho^0/\omega/\phi \to e^+e^-$ and $\eta/\eta' \to e^+e^-\gamma$. In the simulations, QED radiative corrections are provided by PHOTOS [30]. The branching fractions are taken from Ref. [34], except for the unknown $\mathcal{B}(D^0 \to K^-\pi^+\eta)$, which is estimated to be $(1.8 \pm 0.9)\%$ from the related decay $D^0 \to K^0_S\pi^0\eta$. After applying the selection criteria, we expect to find 0.3 ± 0.2 $e^+e^-\gamma$ background decays in the $0.675 < m(e^+e^-) < 0.875\ \mathrm{GeV}/c^2$ range.

The fitted yield for the $D^0 \to K^-\pi^+\pi^+\pi^-$ normalization data sample is 260870 ± 520. For the $D^0 \to K^-\pi^+e^+e^-$ signal mode, the fitted yield, after the subtraction of the $e^+e^-\gamma$ background, is 68 ± 9 in the range $0.675 < m(e^+e^-) < 0.875\ \mathrm{GeV}/c^2$. The significance $S = \sqrt{-2\Delta \ln \mathcal{L}}$ of the signal yield in this mass range, including statistical and systematic uncertainties, is 9.7 standard deviations (σ), where $\Delta \ln \mathcal{L}$ is the change in the log-likelihood from the maximum value to the value when the number of $D^0 \to K^-\pi^+e^+e^-$ signal decays is set to $N_{\mathrm{sig}} = 0$.

Figure 1 shows the results of the fit to the $m(K^-\pi^+e^+e^-)$ and Δm distributions of the $D^0 \to K^-\pi^+e^+e^-$ signal mode in the mass range $0.675 < m(e^+e^-) < 0.875\ \mathrm{GeV}/c^2$. Figure 2 shows the projection of the fit to the $D^0 \to K^-\pi^+e^+e^-$ signal mode as a function of $m(e^+e^-)$ and $m(K^-\pi^+)$, where the background has been subtracted using the *sPlot* technique [37]. A peaking structure is visible in $m(e^+e^-)$ centered near the ρ^0 mass. A broader structure is seen in $m(K^-\pi^+)$ near the known mass of the $\bar{K}^*(892)^0$ meson. Both distributions are similar to the distributions shown in Ref. [21] for the decay $D^0 \to K^-\pi^+\mu^+\mu^-$.

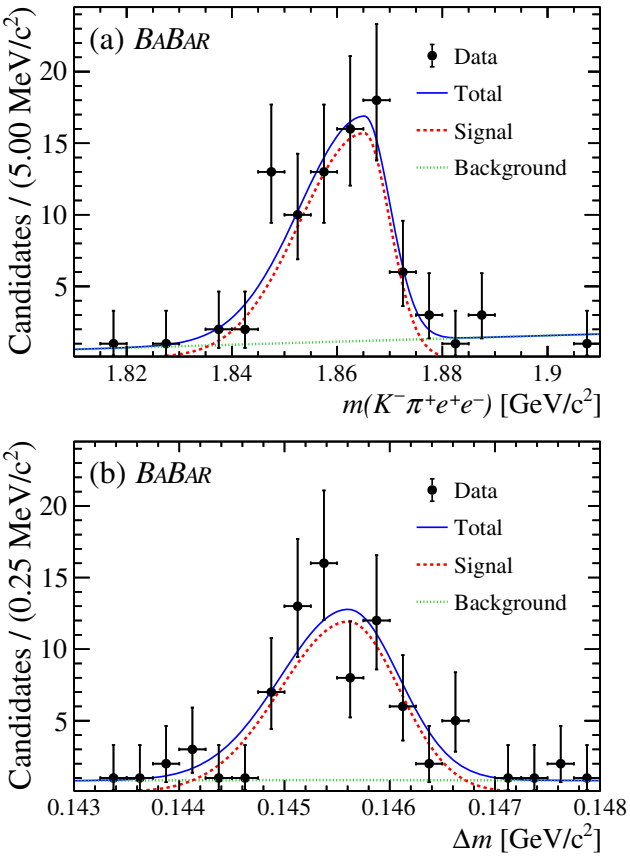

FIG. 1. Fits to $D^0 \to K^-\pi^+e^+e^-$ data distributions for (a) $m(K^-\pi^+e^+e^-)$ and (b) Δm mass for candidates with $0.675 < m(e^+e^-) < 0.875\ \mathrm{GeV}/c^2$.

We test the performance of the maximum likelihood fit by generating ensembles of MC simulation pseudodata samples from both the PDF distributions and the fully simulated MC events. The mean number of signal, normalization, and background yields used in the ensembles is taken from the fits to the data sample. The yields are allowed to fluctuate according to a Poisson distribution and all fit parameters are allowed to vary. No significant bias is observed in the normalization mode. The largest fit bias observed in the signal mode is 0.4 ± 0.1. The biases are much smaller than the statistical uncertainties in the yields. The fit biases are subtracted from the fitted yields before calculating the signal branching fractions.

To cross-check the normalization procedure, the signal mode $D^0 \to K^-\pi^+e^+e^-$ in Eq. (1) is replaced with the decay $D^0 \to K^-\pi^+$, which has a well-known branching fraction [34]. The $D^0 \to K^-\pi^+$ decay is selected using the same criteria as used for the $D^0 \to K^-\pi^+\pi^+\pi^-$ mode, which is used as the normalization mode. The $D^0 \to K^-\pi^+$ yield is determined using an unbinned maximum likelihood fit to Δm and the two-body invariant mass $m(K^-\pi^+)$. Three Crystal Ball functions [38] with shared means are used for the $D^0 \to K^-\pi^+$ signal Δm and $m(K^-\pi^+)$ distributions. The backgrounds are represented

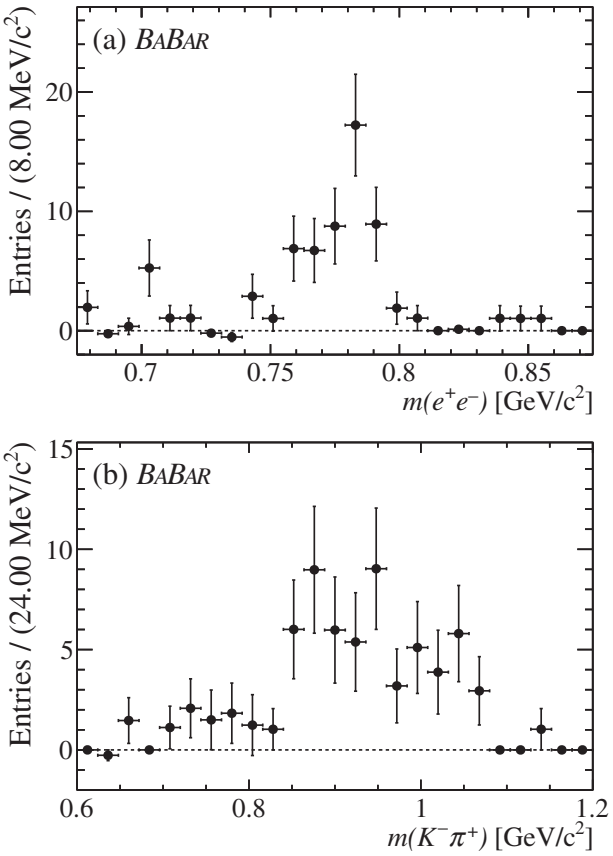

FIG. 2. Projections of the fits to the $D^0 \to K^-\pi^+e^+e^-$ data distributions onto (a) $m(e^+e^-)$ and (b) $m(K^-\pi^+)$ for candidates with $0.675 < m(e^+e^-) < 0.875$ GeV/c^2. The background has been subtracted using the *sPlot* technique [37].

by an ARGUS function for Δm and a second-order Chebyshev polynomial for $m(K^-\pi^+)$. The $D^0 \to K^-\pi^+$ signal yield is 1881950 ± 1380 with an average reconstruction efficiency of $\hat{\epsilon}_{\rm sig} = (27.4 \pm 0.2)\%$. We determine $\mathcal{B}(D^0 \to K^-\pi^+) = (3.98 \pm 0.08 \pm 0.10)\%$ using Eq. (1), where the uncertainties are statistical and systematic, respectively; the current world average is $(3.89 \pm 0.04)\%$ [34]. Similar compatibility with the $\mathcal{B}(D^0 \to K^-\pi^+)$ world-average, but with larger uncertainties, is achieved when the normalization mode $D^0 \to K^-\pi^+\pi^+\pi^-$ in Eq. (1) is replaced with the four-body decay modes $D^0 \to K^-K^+\pi^+\pi^-$ or $D^0 \to \pi^-\pi^+\pi^+\pi^-$.

The main sources of systematic uncertainty are associated with the model parametrizations used in the fits and the normalization procedure, signal MC model, fit bias, tracking and PID efficiencies, luminosity, backgrounds from intermediate decays to $e^+e^-\gamma$, and the normalization mode branching fraction. Some of the tracking and PID systematic effects cancel in the branching fraction determination since they affect both the signal and normalization modes.

Systematic uncertainties associated with the model parametrization are estimated by repeating the fit with the $D^0 \to K^-\pi^+e^+e^-$ signal parameters for the Δm and four-body distributions fixed to values taken from simulation. Alternative fits are also performed with the default peaking and background functions for the signal and normalization modes replaced with alternative functions. The resulting uncertainties are 1.9% and 1.0% for the signal and normalization yields, respectively.

In the mass range $0.675 < m(e^+e^-) < 0.875$ GeV/c^2, we replace the signal phase-space simulation model with a model assuming $D^0 \to \bar{K}^*(892)^0\rho^0$ with $\bar{K}^*(892)^0 \to K^-\pi^+$ and $\rho^0 \to e^+e^-$ and assign half the difference with the default reconstruction efficiency as a systematic uncertainty, equivalent to a relative change of 1.8%. We also use this number as an estimate of the relative change in other regions of $m(e^+e^-)$ and $m(K^-\pi^+)$ where no suitable alternative simulation model exists.

The systematic uncertainty in the fit bias for the signal yield is taken from the ensemble of fits to the MC pseudodata samples and we attribute a value of half the largest fit bias found, ± 0.2. To account for imperfect knowledge of the tracking efficiency, we assign an uncertainty of 0.8% per track for the leptons and 0.7% for the kaon and pion [39]. For the PID, we estimate an uncertainty of 0.7% per electron, 0.2% per pion, and 1.1% per kaon [26]. A systematic uncertainty of 0.8% is associated with the knowledge of the luminosity ratio, $\mathcal{L}_{\rm norm}/\mathcal{L}_{\rm sig}$ [25].

The overall systematic uncertainty in the yields is 5.3% for the signal and 3.6% for the normalization mode. As the PID and tracking systematic uncertainties of the kaons and pions are correlated and cancel, the combined systematic uncertainty in the $D^0 \to K^-\pi^+e^+e^-$ branching fraction is 3.8%, where the uncertainty in the $D^0 \to K^-\pi^+\pi^+\pi^-$ branching fraction is excluded [34].

The branching fraction $\mathcal{B}(D^0 \to K^-\pi^+e^+e^-)$ in the mass range $0.675 < m(e^+e^-) < 0.875$ GeV/c^2 is determined to be $(4.0 \pm 0.5 \pm 0.2 \pm 0.1) \times 10^{-6}$, where the first uncertainty is statistical, the second systematic, and the third comes from the uncertainty in $\mathcal{B}(D^0 \to K^-\pi^+\pi^+\pi^-)$ [34]. This result is compatible within the uncertainties with $\mathcal{B}(D^0 \to K^-\pi^+\mu^+\mu^-)$ reported in Ref. [21].

In the region $0.1 < m(e^+e^-) < 0.2$ GeV/c^2, the fitted signal yield is 175 ± 14, with the distribution dominated by the decay $D^0 \to K^-\pi^+\pi^0$, $\pi^0 \to e^+e^-\gamma$, where the photon has not been reconstructed.

Figure 3 shows the projection of the signal yield as a function of $m(e^+e^-)$ for the fit to Δm and $m(K^-\pi^+e^+e^-)$ in the mass range $m(e^+e^-) > 0.2$ GeV/c^2 above the $\pi^0 \to e^+e^-\gamma$ decay region, where the background has been subtracted using the *sPlot* technique.

We determine the signal yield in the region of the ϕ meson by repeating the fit to Δm and $m(K^-\pi^+e^+e^-)$ with the $m(e^+e^-)$ distribution restricted to the mass range $1.005 < m(e^+e^-) < 1.035$ GeV/c^2. This range corresponds to ± 3 times the ϕ mass width, based on simulation and taking into account the detector resolution. The fitted

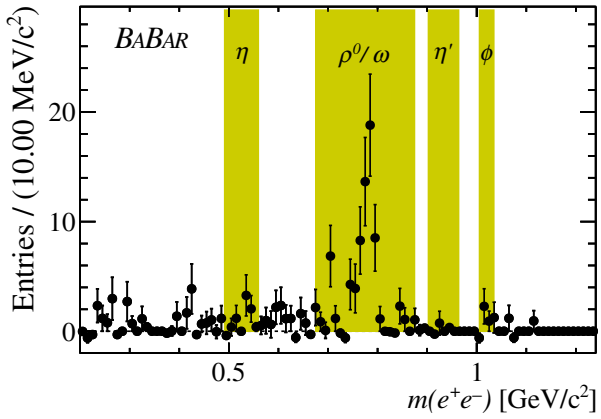

FIG. 3. Projection of the fits to the $D^0 \to K^-\pi^+e^+e^-$ data distributions onto $m(e^+e^-)$ for candidates with $m(e^+e^-) > 0.2\ \mathrm{GeV}/c^2$. The background has been subtracted using the *sPlot* technique [37]. The shaded bands indicate the $m(e^+e^-)$ regions excluded from the "continuum" region.

yield is $3.8^{+2.7}_{-1.9}$, where the uncertainty is statistical only; the statistical significance S is 1.8σ. The branching fraction is determined to be $(2.2^{+1.5}_{-1.1} \pm 0.6) \times 10^{-7}$, where the second uncertainty is systematic and is dominated by the uncertainty on the model parametrization. We use the frequentist approach of Feldman and Cousins [40] to determine a 90% C.L. branching fraction upper limit of 0.5×10^{-6}.

We repeat the fit to Δm and $m(K^-\pi^+e^+e^-)$ in the continuum $m(e^+e^-)$ region that is predicted to be relatively unaffected by intermediates states, and is defined by excluding the following $m(e^+e^-)$ mass ranges: $m(e^+e^-) < 0.2\ \mathrm{GeV}/c^2, 0.675 < m(e^+e^-) < 0.875\ \mathrm{GeV}/c^2, 0.491 < m(e^+e^-) < 0.560\ \mathrm{GeV}/c^2, 0.902 < m(e^+e^-) < 0.964\ \mathrm{GeV}/c^2$, and $1.005 < m(e^+e^-) < 1.035\ \mathrm{GeV}/c^2$. These correspond to ranges dominated by the decays of the π^0 and ρ^0/ω mesons or potentially affected by the decays of η, η', and ϕ mesons, respectively. Simulation samples of $D^0 \to K^-\pi^+\eta$ and $D^0 \to K^-\pi^+\eta'$, with $\eta/\eta' \to e^+e^-\gamma$, are used to determine the asymmetric $m(e^+e^-)$ mass ranges centered on the known η and η' masses. These $m(e^+e^-)$ mass ranges exclude 90% of any remaining simulated η and η' candidates that pass the selection criteria. The number of background decays from intermediate states in the continuum region is predicted to be 9.9 ± 0.9, dominated by the decay $\rho^0/\omega \to e^+e^-$ with $m(e^+e^-)$ less than $0.675\ \mathrm{GeV}/c^2$. The fitted yield in the continuum region, after the subtraction of this background, is 19 ± 7, with a statistical significance $S = 2.6\sigma$. This corresponds to a branching fraction $(1.6 \pm 0.6 \pm 0.7) \times 10^{-6}$, where the second uncertainty is systematic and is dominated by our knowledge of the model parametrization. The result is not significant and we determine a 90% C.L. branching fraction upper limit of 3.1×10^{-6}.

In summary, we have presented the first observation of the decay $D^0 \to K^-\pi^+e^+e^-$. The branching fraction in the mass range $0.675 < m(e^+e^-) < 0.875\ \mathrm{GeV}/c^2$ is $(4.0 \pm 0.5 \pm 0.2 \pm 0.1) \times 10^{-6}$, compatible with the result for $\mathcal{B}(D^0 \to K^-\pi^+\mu^+\mu^-)$ [21], and with theoretical predictions for the SM contribution [6] for this mass region. We have placed 90% C.L. branching fraction upper limits on the decay $D^0 \to K^-\pi^+e^+e^-$ in the $m(e^+e^-)$ mass region of the ϕ meson and in $m(e^+e^-)$ mass regions where long-distance effects are potentially small.

We are grateful for the excellent luminosity and machine conditions provided by our PEP-II colleagues, and for the substantial dedicated effort from the computing organizations that support *BABAR*. The collaborating institutions wish to thank SLAC for its support and kind hospitality. This work is supported by DOE and NSF (USA), NSERC (Canada), CEA and CNRS-IN2P3 (France), BMBF and DFG (Germany), INFN (Italy), FOM (Netherlands), NFR (Norway), MES (Russia), MINECO (Spain), STFC (United Kingdom), BSF (USA-Israel). Individuals have received support from the Marie Curie EIF (European Union) and the A. P. Sloan Foundation (USA).

[*] Deceased.
[†] Present address: Wuhan University, Wuhan 430072, China.
[‡] Present address: Università di Bologna and INFN Sezione di Bologna, I-47921 Rimini, Italy.
[§] Present address: University of Huddersfield, Huddersfield HD1 3DH, United Kingdom.
[¶] Present address: University of South Alabama, Mobile, Alabama 36688, USA.
[**] Also at: Università di Sassari, I-07100 Sassari, Italy.

[1] Charge conjugation is implied throughout.
[2] S. L. Glashow, J. Iliopoulos, and L. Maiani, Phys. Rev. D **2**, 1285 (1970).
[3] A. Paul, I. I. Bigi, and S. Recksiegel, Phys. Rev. D **83**, 114006 (2011).
[4] S. Fajfer, S. Prelovšek, and P. Singer, Phys. Rev. D **64**, 114009 (2001).
[5] S. Fajfer, S. Prelovšek, and P. Singer, Phys. Rev. D **58**, 094038 (1998).
[6] L. Cappiello, O. Cata, and G. D'Ambrosio, J. High Energy Phys. 04 (2013) 135.
[7] A. Paul, A. de la Puente, and I. I. Bigi, Phys. Rev. D **90**, 014035 (2014).
[8] G. Burdman, E. Golowich, J. A. Hewett, and S. Pakvasa, Phys. Rev. D **66**, 014009 (2002).
[9] S. Fajfer and S. Prelovšek, Phys. Rev. D **73**, 054026 (2006).
[10] S. Fajfer, N. Košnik, and S. Prelovšek, Phys. Rev. D **76**, 074010 (2007).
[11] J. P. Lees *et al.* (*BABAR* Collaboration), Phys. Rev. D **88**, 072012 (2013).
[12] M. Huschle *et al.* (Belle Collaboration), Phys. Rev. D **92**, 072014 (2015).
[13] Y. Sato *et al.* (Belle Collaboration), Phys. Rev. D **94**, 072007 (2016).
[14] S. Hirose *et al.* (Belle Collaboration), Phys. Rev. Lett. **118**, 211801 (2017).

[15] R. Aaij *et al.* (LHCb Collaboration), Phys. Rev. Lett. **113**, 151601 (2014).
[16] R. Aaij *et al.* (LHCb Collaboration), Phys. Rev. Lett. **115**, 111803 (2015).
[17] R. Aaij *et al.* (LHCb Collaboration), J. High Energy Phys. 08 (2017) 055.
[18] R. Aaij *et al.* (LHCb Collaboration), Phys. Rev. Lett. **120**, 121801 (2018).
[19] R. Aaij *et al.* (LHCb Collaboration), Phys. Rev. Lett. **120**, 171802 (2018).
[20] R. Aaij *et al.* (LHCb Collaboration), Phys. Rev. D **97**, 072013 (2018).
[21] R. Aaij *et al.* (LHCb Collaboration), Phys. Lett. B **757**, 558 (2016).
[22] A. Freyberger *et al.* (CLEO Collaboration), Phys. Rev. Lett. **76**, 3065 (1996).
[23] E. M. Aitala *et al.* (E791 Collaboration), Phys. Lett. B **462**, 401 (1999).
[24] E. M. Aitala *et al.* (E791 Collaboration), Phys. Rev. Lett. **86**, 3969 (2001).
[25] J. P. Lees *et al.* (*BABAR* Collaboration), Nucl. Instrum. Methods Phys. Res., Sect. A **726**, 203 (2013).
[26] B. Aubert *et al.* (*BABAR* Collaboration), Nucl. Instrum. Methods Phys. Res., Sect. A **479**, 1 (2002); **729**, 615 (2013).
[27] D. J. Lange, Nucl. Instrum. Methods Phys. Res., Sect. A **462**, 152 (2001).
[28] B. F. L. Ward, S. Jadach, and Z. Was, Nucl. Phys. B, Proc. Suppl. **116**, 73 (2003).
[29] T. Sjöstrand, Comput. Phys. Commun. **82**, 74 (1994).
[30] P. Golonka and Z. Was, Eur. Phys. J. C **45**, 97 (2006).
[31] S. Agostinelli *et al.* (GEANT4 Collaboration), Nucl. Instrum. Methods Phys. Res., Sect. A **506**, 250 (2003).
[32] J. Allison, K. Amako, J. Apostolakis, H. Araujo, P. Dubois *et al.* (GEANT4 Collaboration), IEEE Trans. Nucl. Sci. **53**, 270 (2006).
[33] I. Adam *et al.*, Nucl. Instrum. Methods Phys. Res., Sect. A **538**, 281 (2005).
[34] M. Tanabashi *et al.* (Particle Data Group), Phys. Rev. D **98**, 030001 (2018).
[35] H. Albrecht *et al.* (ARGUS Collaboration), Phys. Lett. B **241**, 278 (1990).
[36] The Cruijff function is a centered Gaussian with different left-right resolutions and non-Gaussian tails: $f(x) = \exp\{-(x-m)^2/[2\sigma_{L,R}^2 + \alpha_{L,R}(x-m)^2]\}$.
[37] M. Pivk and F. R. Le Diberder, Nucl. Instrum. Methods Phys. Res., Sect. A **555**, 356 (2005).
[38] T. Skwarnicki, A study of the radiative cascade transitions between the Υ' and Υ resonances, Ph.D. thesis, Institute of Nuclear Physics, Krakow, 1986, Report No. DESY-F31-86-02.
[39] T. Allmendinger *et al.*, Nucl. Instrum. Methods Phys. Res., Sect. A **704**, 44 (2013).
[40] G. J. Feldman and R. D. Cousins, Phys. Rev. D **57**, 3873 (1998).